Electrical Power and Energy Systems 100 (2018) 129–138

Contents lists available at ScienceDirect

Electrical Power and Energy Systems

journal homepage: www.elsevier.com/locate/ijepes

# An improved control method for unified power quality conditioner with unbalanced load

Ashish Patel*, H.D. Mathur, Surekha Bhanot

*Department of Electrical and Electronics Engineering, Birla Institute of Technology and Science, Pilani 333031, India*

ARTICLE INFO

*Keywords:*
UPQC
Power quality
Power angle control
Load unbalance

ABSTRACT

This paper proposes an improved control method for Unified Power Quality Conditioner (UPQC) with unbalanced load. In UPQC, shunt APF is overburdened when it alone supplies total load reactive power. PAC method aims at effective utilization of series and shunt APFs by sharing reactive power burden between the two. In presence of unbalanced load, existing PAC methods can lead to circulation of reactive power between two APFs and thereby result in overloading of UPQC. Also, due to unbalanced compensating currents, DC link voltage contains second order oscillations, which deteriorates source current quality. In this work, a new PAC method is proposed, which avoids circulation of reactive power and unnecessary VA burden on UPQC. To suppress DC link voltage oscillations, proposed control employs a 'mean block' (moving average) at output of PI controller, which ensures balanced and harmonic free source currents. Also, a 'percentage unbalance' parameter has been proposed to quantify the unbalance in three phase quantities. Performance of proposed UPQC system is tested in the presence of non-linear, reactive and unbalanced loads. Dynamic performance of system is studied during grid disturbances such as voltage sag, swell, and change in load. Real time simulation carried out in Opal-RT validate the effectiveness of proposed method. The electrical circuit of UPQC is simulated with sub-microsecond time step on FPGA based computational engine of Opal-RT for better verification of the proposed control.

## 1. Introduction

Power quality is one of the major challenges of smart grid [1]. With increasing use of power electronic converters, power quality issues such as harmonic distortions have been increasing rapidly. Active Power Filters (APFs) being dynamic and fast, are preferred over passive filters to compensate for power quality issues. Series APF mainly compensates for supply voltage related power quality problems such as voltage sag, swell and harmonics. On other hand, shunt APF mainly compensates for load current related power quality issues such as poor power factor, unbalance, and harmonics. UPQC (Unified Power Quality Conditioner) is a combination of series and shunt APFs sharing a common DC link. UPQC, integrating benefits of both series and shunt APF, compensates for most of the power quality issues [2].

Shunt APF of UPQC identifies non-linear and out of phase components from load currents and supplies them to load, maintaining balanced, sinusoidal source currents with unity power factor. To achieve this function, many techniques such as Instantaneous Reactive Power Theory (IRPT or p-q theory), Synchronous Reference Frame Theory (SRFT or d-q theory) are used. IRPT based techniques for shunt APF are simple and have been used widely [3,4]. However, IRPT based techniques don't perform well in non-ideal supply voltage conditions, so SRFT based techniques are preferred over IRPT based techniques [5,6]. Apart from comensating for load current based power quality issues, shunt APF also regulates DC link voltage, for which a PI controller is used generally.

Series APF of UPQC monitors supply voltage and detects any non-ideality such as sag, swell or harmonics. These non-ideal components of supply voltages are extracted by series APF and corresponding compensating voltages are injected in series with supply voltages to maintain ideal voltage across load terminals. To accomplish this task, various control techniques are used in literature such as IRPT [1], SRFT [5,7], and Unit Vector Template Generation (UVTG) [8]. UVTG based technique is simple and doesn't require any PI controller [8]. In absence of non-ideality in supply voltage, output voltages of series APF are effectively zero.

VA rating of series APF is under-utilized if it compensates only for transient grid disturbances such as voltage sag and swell, so Power Angle Control (PAC), which aims at effective utilization of VA ratings of series and shunt APF of UPQC, has been proposed [3,9]. In PAC, series APF provides part of load reactive power by injecting voltage at an angle with source current (unlike conventional control, in which series

* Corresponding author.
*E-mail address:* ashish.patel@bits.bits-pilani.ac.in (A. Patel).

https://doi.org/10.1016/j.ijepes.2018.02.035
Received 1 October 2017; Received in revised form 17 January 2018; Accepted 18 February 2018

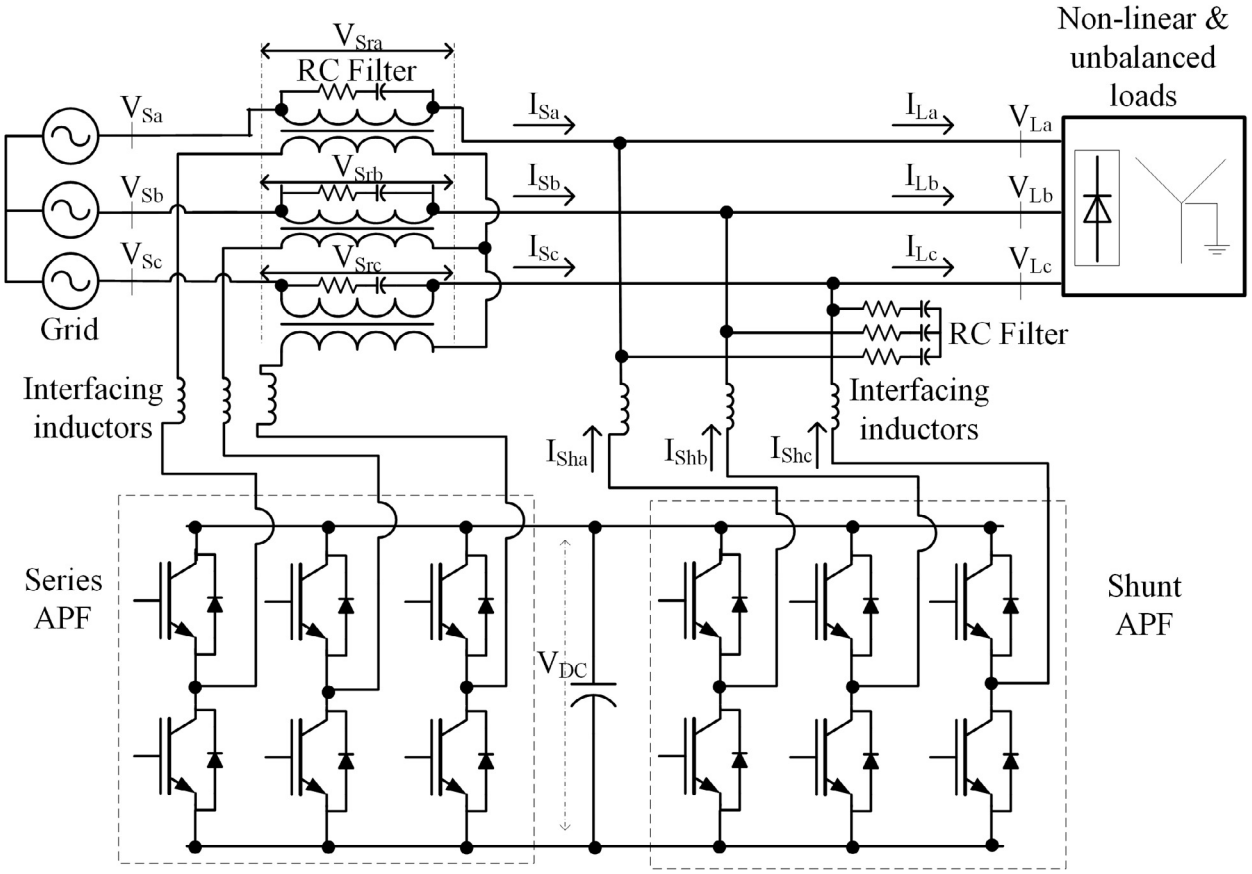


**Fig. 1.** Configuration of 3-phase, 3-wire UPQC.

APF injects voltage in phase with source current). Out of phase injection of series voltage introduces a phase angle, commonly known as power angle, between load voltage and source voltage. During voltage sag or swell, series APF in PAC approach compensates for sag or swell along with providing part of load reactive power either by keeping power angle constant or varying it suitably [4].

In short, control of UPQC involves measurement of source and load voltages and currents, computation of PAC algorithms, on-line generation of reference currents for shunt APF & reference voltages for series APF, and feedback control in these APFs. However, overall performance of UPQC depends on regulation of DC link voltage [10]. In presence of unbalanced loads, shunt APF supplies unbalanced components of load currents, due to which DC link voltage experiences second order oscillations, which eventually affect the performance of UPQC.

Good amount of research has been already carried out on control and performance of UPQC in presence of unbalanced loads [5,11,12], however, little attention is given to DC link voltage oscillations, its effects on performance of UPQC, and solution for it. A sinusoidal integration block is added to remove DC link voltage oscillations in shunt APF with unbalanced load [13], and a proportional resonant controller is used in place of conventional PI controller [14], but these methods are complex, increase computation burden on controller, and have slow dynamic response.

Most of the PAC methods proposed for UPQC, don't account for inherent system non-idealties like distortion is source voltage and unbalance in loads. PAC method of UPQC in works [3,4] is based on IRPT theory (p-q theory), which makes this method sensitive to non-ideal supply voltages. So, SRFT (d-q theory) based PAC method for UPQC has been developed, but sag/swell compensation along with PAC is not considered in control of series APF [15].

SRFT based PAC method, which shares load reactive power equally between series and shunt APF has been developed to achieve equal VA loading of these APFs [16], but method is complex and gives accurate results only with very small values of power angle because load power is calculated in source voltage reference frame, which differs considerably from load voltage reference frame for appreciable value of power angle. PAC methods proposed so far, don't consider DC link voltage oscillations in presence of non-linear loads. Apart from this, in existing PAC methods, unbalanced load can cause circulation of reactive power, which leads to increase in power losses and overloading of UPQC (which is proven theoretically as well as by real time simulation in present work).

In the present work, following improvements are proposed in UPQC control:

- A new PAC method is proposed to avoid circulation of reactive power and associated overloading of UPQC in presence of unbalanced load.
- To minimize effects of DC link voltage oscillations, a 'mean' (moving average) block is added at the output of PI controller. The 'mean' block removes oscillations in current estimated by PI controller, which results in improvement in source current power quality.

Performance of proposed system is tested in steady state as well as in dynamic states using real time digital simulation with help of Opal-RT.

The rest of paper is organized as follows: Section 2 describes configuration of solar PV based UPQC. Section 3 gives mathematical analysis of PAC method of UPQC. Section 4 covers control of UPQC with proposed PAC approach. Section 5 presents simulation test case with methodology, Section 6 discusses results and Section 7 concludes contribution of the paper.

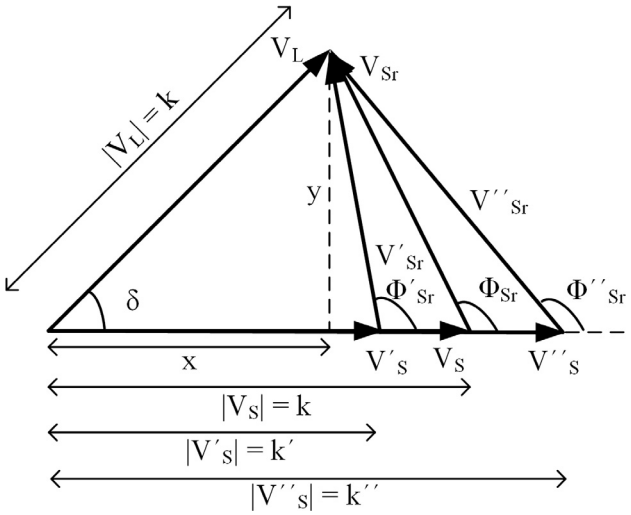


**Fig. 2.** Phasor diagram of UPQC under PAC approach.

## 2. Configuration of UPQC

In this work, configuration of UPQC is based upon three phase three wire supply system, which is most common in distribution system. This configuration has two major components or Power Electronic Converters: shunt APF, and series APF. Both series and shunt APFs are IGBT based three phase three leg bridge inverters sharing a common DC link. Single phase series injection transformers are used in each phase to inject voltage produced by series APF. Interfacing inductors are used at the output of both series and shunt APFs. High pass RC filters are used at the output of series and shunt APFs to filter out high frequency components in voltage or current, generated by PWM switching of these APFs.

## 3. Analysis of PAC method

As mentioned in Section 1, load voltage exhibits a phase shift with respect to source voltage in PAC method of UPQC. Voltage based phasor diagram of PAC approach is shown in Fig. 2. In this figure $V_S$ is nominal supply voltage with its rms value (= $k$). In normal condition load voltage ($V_L$) makes an angle $\delta$ with source voltage with its rms value (= $k$). Series voltage ($V_{Sr}$) injected by series APF is a phasor difference of load voltage and source voltage.

On occurrence of sag, magnitude (rms) of supply voltage is reduced to $k'$. If power angle ($\delta$) is held fixed then series voltage ($V'_{Sr}$) injected during sag will have less magnitude than $V_{Sr}$ injected during normal operation. Reverse is the case when swell occurs on the system. During swell, series voltage ($V''_{Sr}$) has highest magnitude among three cases as shown in Fig. 2. Thus, if fixed power angle method is used, then rating of series APF should be selected based on maximum swell condition. The disadvantage of this approach is that since swell occurrence is rare, series APF rating will be under utilized during normal operation.

In variable PAC method, $\delta$ value is changed when sag or swell occurs. Series APF operates at its full rating during normal operation if there is sufficient demand of reactive power from load. On occurrence of sag or swell this power angle is changed in such a way that series APF still operates at its full capacity. From Fig. 2 following equations can be derived under sag condition:

$$x = k\cos\delta \tag{1}$$

$$y = k\sin\delta \tag{2}$$

$$|V'_{Sr}| = \sqrt{y^2 + (k'-x)^2} \tag{3}$$

$$|V'_{Sr}| = \sqrt{k^2 + k'^2 - 2kk'\cos\delta} \tag{4}$$

Assuming $f_S$ to be fraction of voltage sag, and $f_{Sr}$ to be ratio of series voltage ($V'_{Sr}$) to rated source voltage $k$. Further simplifications can be made and equation for delta can be obtained as below:

$$f_S = k'/k \tag{5}$$

$$f_{Sr} = |V'_{Sra}|/k \tag{6}$$

$$f_{Sr} = \sqrt{1 + f_S^2 - 2f_S\cos\delta} \tag{7}$$

$$\delta = \cos^{-1}\left[\frac{1 + f_S{}^2 - f_{Sr}^2}{2f_S}\right] \tag{8}$$

From (8) it can be observed that if series APF is supplying rated voltage ($V_{Sr,max}$) then $\delta$ will be at its maximum value at a particular supply voltage. So, for a value of supply voltage ($V_S$), maximum value of power angle can be calculated:

$$\delta_{max} = \cos^{-1}\left[\frac{1 + f_S{}^2 - f_{Sr,max}^2}{2f_S}\right] \tag{9}$$

It's important to note is that $\delta_{max}$ is not a fixed value, rather it varies with variation in supply voltage due to presence of $f_S$ in Eq. (9). Actual value of $\delta$ in case of normal UPQC is calculated from reactive power ($Q_{Sr}$) supplied by series APF and load active power ($P_L$) using Eq. (10) [3].

$$\delta = \sin^{-1}\left(\frac{Q_{Sr}}{P_L}\right) \tag{10}$$

Maximum reactive power handled by series APF under normal supply voltage conditions can be computed using Eq. (11). Rest of the reactive power demand of load is to be supplied by shunt APF of UPQC.

$$Q_{Sr,max} = P_L\sin\delta_{max} \tag{11}$$

Equal reactive power sharing between shunt and series APFs proposed in [16] works fine with balanced loads, but while compensating for unbalanced loads it can lead to circulation of reactive power between series and shunt APFs of UPQC. During the circulation, one APF supplies reactive power and another APF consumes a part of it, and remaining part goes to load. So total reactive power dealt by of both APFs exceeds load reactive power. This leads to increased VA loading of UPQC. Also, power losses increase due to circulation of currents. How equal reactive power sharing leads to circulation of reactive power can be understood by following mathematical derivation:

Let $Q_{La}$, $Q_{Lb}$, $Q_{Lc}$ be three phase reactive power demands of an unbalanced load. Total reactive power of load will be sum of all these (Eq. (12)). While sharing reactive power equally, series APF will supply half of $Q_T$ (Eq. (13)). Since series APF can supply only balanced power, each phase of it will supply $Q_T/6$ (Eq. (14)).

$$Q_T = Q_{La} + Q_{lb} + Q_{Lc} \tag{12}$$

$$Q_{Sr} = Q_T/2 \tag{13}$$

$$Q_{Sra} = Q_{Srb} = Q_{Src} = Q_T/6 \tag{14}$$

Reactive power supplied by shunt APF in each phase will be difference of load reactive power and series APF power in that phase:

$$Q_{Sha} = Q_{La} - Q_T/6 \tag{15}$$

$$Q_{Shb} = Q_{Lb} - Q_T/6 \tag{16}$$

$$Q_{Shc} = Q_{Lc} - Q_T/6 \tag{17}$$

Let $Q_{La}$ be the least among three phase load reactive powers, then balanced reactive power is given by Eq. (18). If load is sufficiently unbalanced then balanced reactive power will be less than half of total reactive power as given by inequality Eq. (19), due to which, $Q_{Sha}$ will be negative meaning shunt APF will consume reactive power in phase A, since series APF supplies more reactive power than required. So

circulation of reactive power will take place between two APFs.

$$Q_{Bal} = 3Q_{La} \tag{18}$$

$$3Q_{La} < Q_T/2 \tag{19}$$

When considering total VA power burden on UPQC, magnitude of reactive powers of series and shunt APFs are added. Since $Q_{Sha}$ is negative, its magnitude will be $-Q_{Sha}$. Neglecting active power injections, VA burden of UPQC will be given by Eq. (20) and simplified in Eq. (21).

$$VA_{UPQC} = (Q_T/6-Q_{La}) + (Q_{Lb}-Q_T/6) + (Q_{Lc}-Q_T/6) + Q_T/2 \tag{20}$$

$$VA_{UPQC} = (Q_T/3-Q_{La}) + Q_{Lb} + Q_{Lc} \tag{21}$$

$$Q_T/3-Q_{La} > Q_{La} \tag{22}$$

$$VA_{UPQC} > Q_{La} + Q_{Lb} + Q_{Lc} \tag{23}$$

From inequality Eq. (19), inequality Eq. (22) can be derived, which proves that $VA_{UPQC}$ is greater than load reactive power (Eq. (23)). So, with unbalanced load, PAC approach of UPQC requires special consideration, which is taken up in this work.

## 4. Control of UPQC using PAC approach

In UPQC, shunt APF compensates for current based power quality issues by injecting appropriate current into system and series APF compensates for voltage based power quality issues by injecting suitable voltage in series with source voltage. So shunt APF acts as a current source, and series APF acts as a voltage source. Shunt APF also performs task of DC link voltage regulation. Details of control of each of these converters are described in following subsections.

### 4.1. Shunt APF control

Shunt APF of UPQC injects compensating currents for mitigating load current based power quality issues and handles current required for maintaining DC link voltage (Fig. 3). SRF theory based extraction method is used for generating reference signals corresponding to compensating currents. In SRF based extraction, three phase load currents are transformed from abc frame to dq0 frame using Park's transform (1), and *wt* signal required for this transformation is generated using a three phase PLL on source voltages.

$$\begin{bmatrix} I_d \\ I_q \\ I_0 \end{bmatrix} = \frac{2}{3}\begin{bmatrix} \cos wt & -\sin wt & 1/2 \\ \cos\left(wt-\frac{2\pi}{3}\right) & -\sin\left(wt-\frac{2\pi}{3}\right) & 1/2 \\ \cos\left(wt+\frac{2\pi}{3}\right) & -\sin\left(wt+\frac{2\pi}{3}\right) & 1/2 \end{bmatrix}\begin{bmatrix} I_{La} \\ I_{Lb} \\ I_{Lc} \end{bmatrix} \tag{24}$$

Park's transform converts fundamental components of AC quantities into DC quantities which are easily extracted using low pass filters. Current needed for maintaining DC link voltage is estimated using a PI controller and added to d-axis load current. The resultant current is d-axis reference source current $I_d^*$, which is transformed into three phase balanced sinusoidal reference source currents using inverse Park's transform. Reference and measured source currents are passed through a hysteresis controller to generated switching pulses for shunt APF.

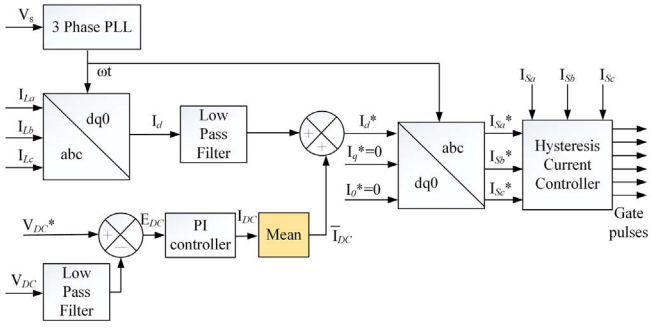


**Fig. 3.** Control of shunt APF.

While compensating for unbalanced load, shunt APF supplies unbalanced currents, which leads to second order ripples in DC link voltage. These ripples pass through PI controller and are reflected in $I_d^*$, due to which reference and actual source currents become unbalanced. Therefore, present work proposes use of a mean (moving average) block, which computes mean of input signal continuously using a running window of predefined frequency. Using mean block at the output of PI controller suppresses these ripples and prevents them from passing onto $I_d^*$. One can think of using low pass lifter also, but that leads to slow transient response.

Effectiveness of the mean block in minimizing second order ripples in $I_d^*$ can be proven mathematically. Let $E_{DC}(t)$ be error input to PI controller. In presence of unbalanced load, $E_{DC}(t)$ will contain second order ripples:

$$E_{DC}(t) = E_0 + E_2\cos(\omega_2 t + \phi_2) \tag{25}$$

First term in Eq. (25) represents DC component in the error and second term represents ripple component of second order. Current required to maintain DC link voltage ($I_{DC}(t)$) is estimated by PI controller:

$$I_{DC}(t) = K_P E_{DC}(t) + K_I \int_0^t E_{DC}(\tau)d\tau \tag{26}$$

From Eqs. (25) and (26), following equation can be obtained:

$$I_{DC}(t) = K_P E_0 + K_I \int_0^t E_0 d\tau + K_P E_2\cos(\omega_2 t + \phi_2) + K_I \int_0^t E_2\cos(\omega_2\tau + \phi_2)d\tau \tag{27}$$

$$I_{DC}(t) = K_P E_0 + K_I \int_0^t E_0 d\tau + K_P E_2\cos(\omega_2 t + \phi_2) + \frac{K_I E_2[\sin(\omega_2\tau + \phi_2)-\sin\phi_2]}{\omega_2} \tag{28}$$

It is clearly seen from Eq. (28) that $I_{DC}$ contains second order ripples, which were present in error input of PI controller. If no mean block is used, then these ripples are propagated to $I_d^*$ and deteriorate reference source currents. When mean block (of frequency $\omega$) is used, then mean of DC link current over a running window of $2\pi/\omega$ is given by Eq. (29):

$$\bar{I}_{DC}(t) = \frac{1}{2\pi/\omega}\int_t^{t+2\pi/\omega}\left[K_P E_0 + K_I \int_0^t E_0 d\tau - \frac{K_I E_2\sin\phi_2}{\omega_2}\right]dt + \frac{1}{2\pi/\omega}\int_t^{t+2\pi/\omega}\left[K_P E_2\cos(\omega_2 t + \phi_2) + \frac{K_I E_2\sin(\omega_2\tau + \phi_2)}{\omega_2}\right]dt \tag{29}$$

Second term in Eq. (29) represents ripples, and it vanishes when $\omega = \omega_2$, since integration of a sinusoidal quantity over its time period is zero. So, A mean block at frequency equal to ripple frequency of DC link, eliminates ripples from $I_{DC}$ and finally, $I_d^*$ also becomes free ripples.

### 4.2. Series APF control

In PAC approach, series APF injects suitable series voltage to compensate for power quality issues in supply voltage and to supply a part of load reactive power. In order to supply a part of load reactive power series voltage should be injected at a particular angle with supply current, resulting in phase difference between load voltage and supply voltage. For generating reference signals for series APF, load voltage phase angle (power angle) with respect to source current/voltage needs to be estimated.

#### 4.2.1. Estimation of power angle

Block diagram for estimation of power angle is shown in Fig. 4. Load active and reactive powers in each are computed using single phase

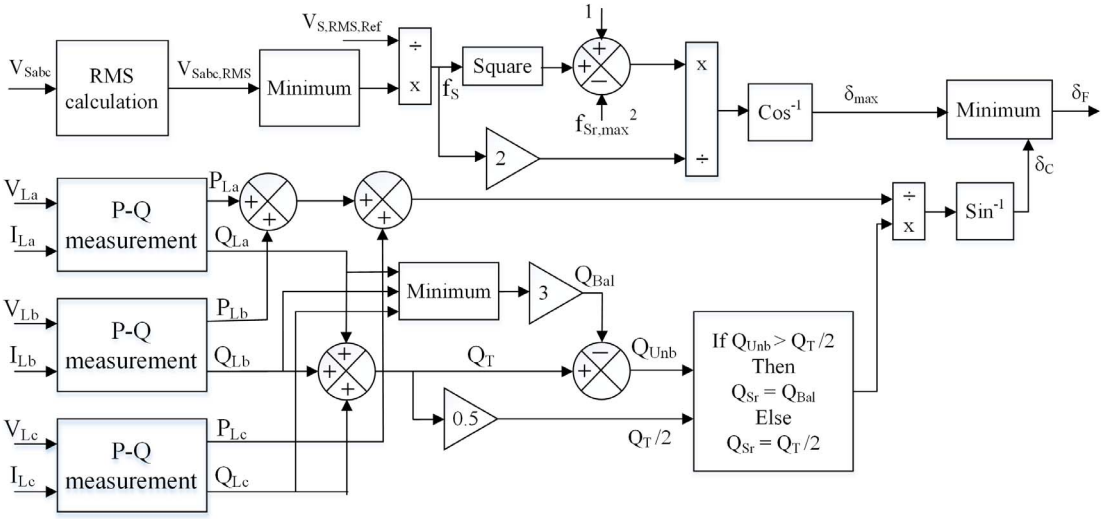


**Fig. 4.** Estimation of instantaneous power angle ($\delta$).

Fourier transform based P-Q measurement blocks. Balanced load reactive power is computed by tripling minimum reactive power in a phase. Unbalanced reactive power is found by reducing balanced reactive power from total. Unbalanced reactive power is compared with half of total reactive power. If unbalanced reactive power is less than or equal to half of total reactive power then there is no scope for power circulation (as it is already proven in Section 3), and equal reactive power is shared equally between series and shunt APFs.

When unbalanced reactive power is more than half of the total reactive power then series APF supplies only balanced reactive power. Remaining reactive power (unbalanced) is supplied by shunt APF. This method avoids circulation of reactive power and overloading of UPQC. Once reactive power supplied by series APF is decided, power angle ($\delta_C$) is calculated accordingly using Eq. (10) (While using Eq. (10), a limiter is used to avoid division by zero).

Since maximum power angle ($\delta_{max}$) varies with supply voltage, it's value is calculated instantaneously using Eq. (9) (In this equation also a limiter is used to avoid denominator becoming zero). For implementing Eq. (9), first RMS values of three phase supply voltages are computed and minimum of them is divided by reference RMS value to find fraction $f_S$. Maximum amount of sag or swell compensated by series APF decides $f_{Sr,max}$. Finally Eq. (9) is implemented for estimating $\delta_{max}$ from values of $f_S$ and $f_{Sr,max}$. Finally calculated power angle ($\delta_C$) is compared to $\delta_{max}$ and minimum of the two is selected as final $\delta_F$ for control of series APF.

#### 4.2.2. Control method of series APF

Control of Series APF is implemented using Unit Vector Template Generation (UVTG) technique [8]. This technique is simple and reduces the computation burden on the controller. In this technique no PI controller is required as evident from Fig. 5. Thus, PI tuning is also not required, which saves design effort. A three phase PLL (Phase Locked Loop) is used to generate *wt* corresponding to phase A (reference phase) fundamental component of source voltage. This *wt* is then added with $\delta_F$ estimated using power angle estimator block, and their sum is used to generate three phase balanced unit vectors (time varying sinusoidal signals with unit amplitude) using Eq. (30).

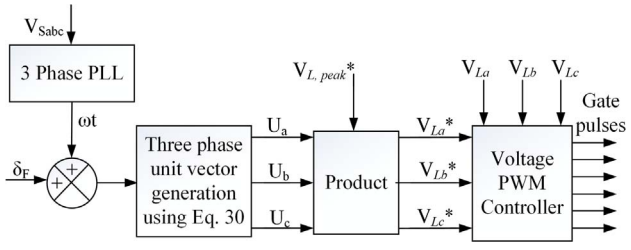


**Fig. 5.** Control of series APF.

$$\begin{bmatrix} U_a \\ U_b \\ U_c \end{bmatrix} = \begin{bmatrix} \sin(wt + \delta_F) \\ \sin(wt + \delta_F - 2\pi/3) \\ \sin(wt + \delta_F + 2\pi/3) \end{bmatrix} \quad (30)$$

The desired (reference) amplitude of load voltage is multiplied with these unit vectors to generate reference load voltage signals, which are phase displaced from source voltages by angle $\delta_F$. Sensed load voltage signals and reference load voltage signals are then fed to voltage PWM controller of series APF.

## 5. Simulation data and methodology

Real time simulation has been an effective way of validating power electronic circuits [17]. Since electrical circuits have fast response they require smaller time step than their control circuit. Thus real time co-simulation provides a better performance evaluation method. In this work real time simulator Opal-RT OP4510 has been used for testing performance of proposed UPQC. This simulator has two processing units: Central Processing Unit (CPU) core, and Field Programmable Gate Array (FPGA) computational engine.

Electrical circuit part of UPQC is simulated on FPGA engine of Opal-RT with time step of 0.5 μs, and proposed control algorithms are implemented on its CPU core with 15 μs time step (Fig. 6). FPGA based computational engines provide much small time steps for accurate and detailed modeling of power electronic circuits [18]. CPU and FPGA communicate with each other synchronously through Peripheral Component Interconnect (PCI) bus of simulator. CPU sends control signals (PWM pulses for switches) to circuit simulated on FPGA in response to measurements coming to CPU from FPGA.

For real time simulation, MATLAB/Simulink model of proposed system is used. The control and electrical circuit of the model are separated and implemented on CPU core and FPGA engine of Opal-RT hardware through RT-Lab software. After simulation the recorded results are sent from Opal-RT simulator to host PC for analysis. Alternatively, after suitable scaling, the simulation results can be obtained on analog output channels of simulator and can be stored using Digital Storage Oscilloscope (Keysight MSO-X 3034A).

Parameters of UPQC system shown in Fig. 1 are calculated using procedure elaborated in [7] and the selected values of these parameters are shown in Table 1. Three phase grid supply is selected as 415 V,

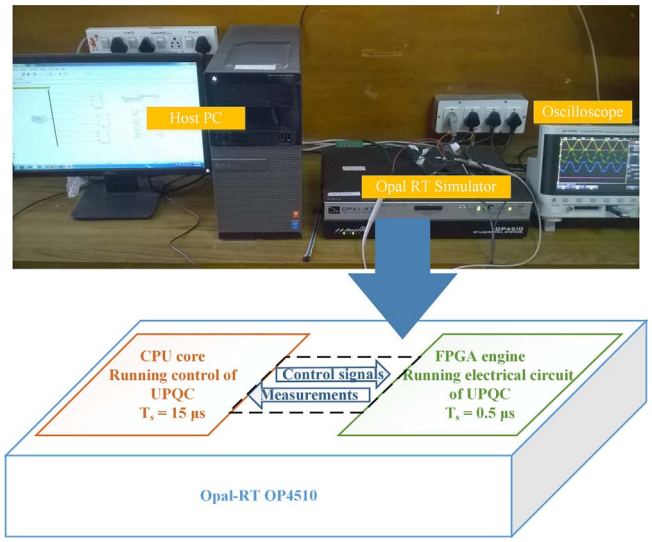


**Fig. 6.** Real time simulation framework.

**Table 1**
Parameters of UPQC

| | |
|---|---|
| 3 Phase supply | 415 V, 50 Hz, $R_S$ = .1 Ω, $L_S$ = 0.5 mH |
| DC link | $V_{DC}$ = 700 V, $C_{DC}$ = 5500 µF |
| Shunt APF | $L_{Sh}$ = 1.0 mH |
| Series APF | $L_{Sr}$ = 3.0 mH, $n_T$ = 1, $S_T$ = 2.5 kVA |
| Load-1 | diode bridge rectifier ($R_{DC}$ = 20 Ω) |
| Load-2 | $R_Y$ = 8 Ω/phase, $L_Y$ = 5 mH/phase |
| Load-3 | $R_{ca}$ = 8 Ω, $L_{ca}$ = 40 mH |

50 Hz with source resistance $R_S$ and inductance $L_S$. Load-1 is a three phase diode rectifier based non-linear load, supplying a DC load, which is a resistance of value $R_{DC}$. Load-2 is a liner star connected load with per phase resistance $R_Y$ and per phase inductance $L_Y$. Load-3 is a series combination of resistance $R_{ca}$ and inductance $L_{ca}$, connected between phase a and phase c.

For UPQC system dc link voltage $V_{DC}$, and capacitor $C_{DC}$ values are selected as shown in Table 1. $L_{Sh}$ and $L_{Sr}$ are AC interfacing inductors used for connecting shunt and series APFs. Among parameters of series APF, $n_T$ and $S_T$ are turns ratio and kVA rating of each series injection transformer.

## 6. Results and discussion

Steady state performance of proposed control scheme is studied in presence of all three types of loads: linear, non-linear, and unbalanced. For evaluating dynamic response, proposed UPQC system is simulated for three cases covering sag in supply voltage, swell in supply voltage and change in load. These cases are further described in following subsections.

### 6.1. Steady state performance

Under steady state operation, all three loads are connected and UPQC is operating under PAC method, sharing reactive power burden of load between series and shunt APFs. Load currents ($I_L$) are unbalanced due to presence of load-3 (Fig. 7a). They also contain harmonics due to non-linear load (load-1). Shunt APF injects suitable compensating currents ($I_{Sh}$) and maintains sinusoidal, balanced supply currents ($I_S$). Total Harmonic Distortion (THD) value of load current is 10.51% and that of source current is 3.77% (FFT spectrum is shown in Appendix A). Since shunt APF supplies unbalanced currents, DC link voltage contains second order ripples (Fig. 7b).

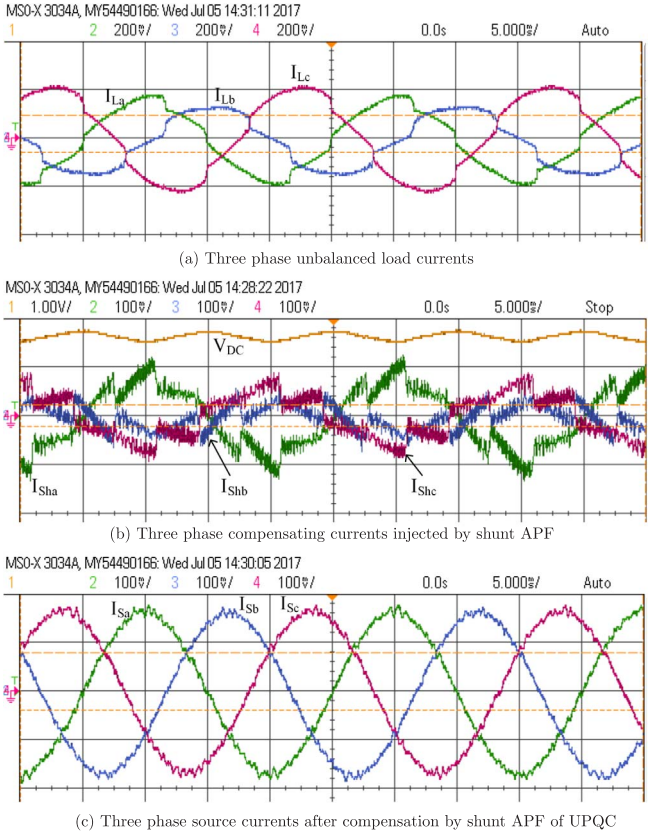


**Fig. 7.** Current waveforms in steady state of UPQC. Scale – $I_S$: 50 A/div., $I_L$: 100 A/div., $I_{Sh}$: 50 A/div., $V_{DC}$: 50 V/div., time: 5 ms/div.

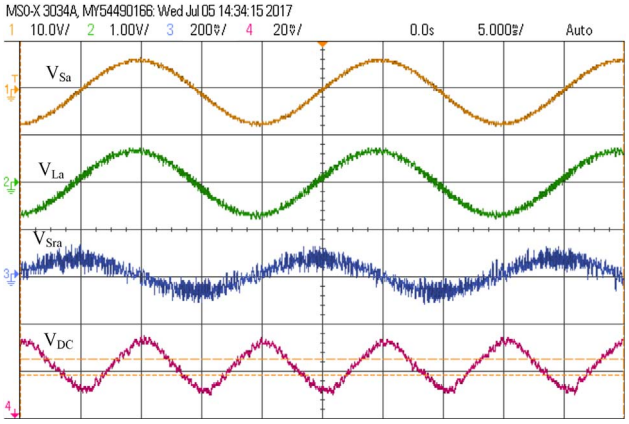


**Fig. 8.** Voltage waveforms in steady state of UPQC. Scale – $V_{Sa}$: 500 V/div., $V_{La}$: 500 V/div., $V_{Sra}$: 100 V/div., $V_{DC}$: 10 V/div., time: 5 ms/div.

Voltage waveforms in steady state are shown in Fig. 8. Since voltages are balanced, only phase A waveforms are shown. Phase difference (power angle) between source voltage ($V_{Sa}$) and load voltage ($V_{La}$) can be observed in Fig. 9. The value of power angle is found to be 6.2°. Due to such small value of power angle, phase difference between load and source voltages is not clearly evident. Source voltage and current are in phase confirming unity power factor at source. Voltage injected by series APF is at suitable phase angle with source current to yield required power angle of 6.2° between supply and load voltages. It can also be observed that series voltage ($V_{Sra}$) is almost in quadrature with source current, indicating that series APF mainly injects reactive power with negligible active power exchange to meet power losses.

Comparison of steady state performance of proposed method is carried with method used in [16], which is considered as base case. In base case, no

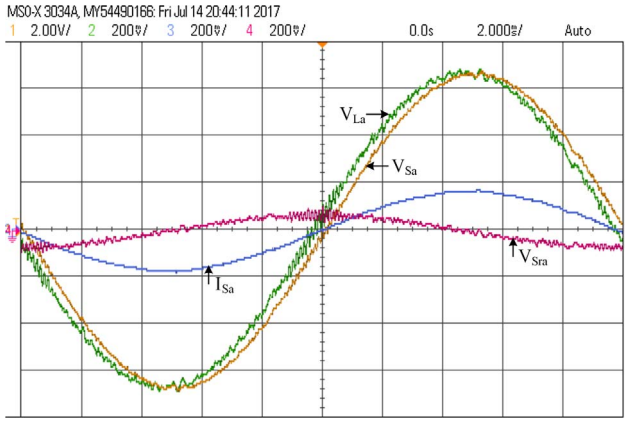


**Fig. 9.** Phase difference between key voltages and currents. Scale – $V_{Sa}$: 100 V/div., $V_{La}$: 100 V/div., $V_{Sra}$: 100 V/div., $I_{Sa}$: 100 A/div., time: 2 ms/div.

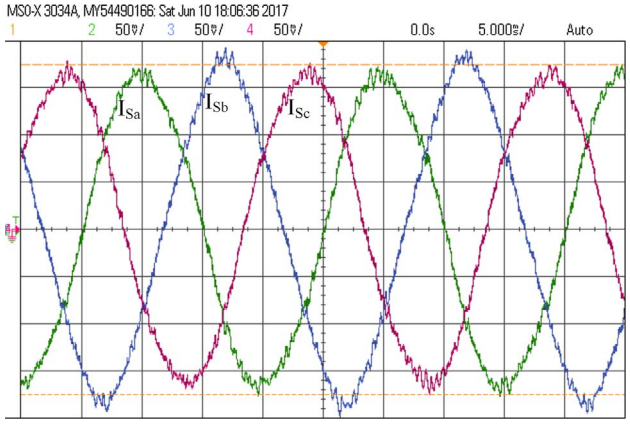


**Fig. 10.** Source currents waveforms using method proposed in [16] (Base Case, without mean block). Scale – $I_{Sa}$: 50 A/div., $I_{Sb}$: 50 A/div., $I_{Sc}$: 50 A/div., time: 5 ms/div.

**Table 2**
Comparison of source current power quality using different control methods.

| S.N. | Method description | Percentage unbalance in $I_s$ | THD of $I_s$ |
|---|---|---|---|
| 1 | No compensation (without UPQC) | 27.93% | 10.51% |
| 2 | Base case (without mean block, [16]) | 2.66% | 4.38% |
| 3 | Proposed control (with mean block) | 0.11% | 3.59% |

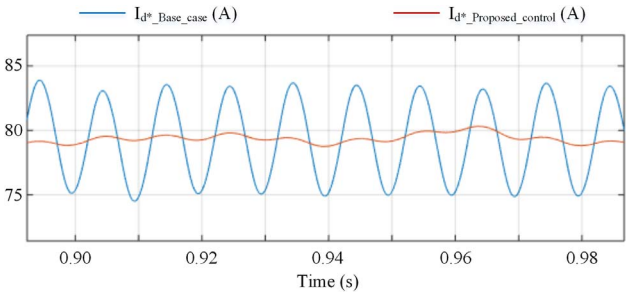


**Fig. 11.** Reference d-axis current waveforms in base case (without mean block) and proposed control (with mean block).

mean block is used at the output of PI controller and load reactive power is shared equally between series and shunt APF, even in presence of unbalanced load. This comparison is based on two criteria- (1) power quality of source currents and (2) Overall VA burden on UPQC while supplying

**Table 3**
Comparison of VA loading of UPQC with unbalanced load

| S.N. | Method description | kVAr &(kVA) load on shunt APF | kVAr &(kVA) load on series APF | kVA load on UPQC |
|---|---|---|---|---|
| 1 | Base case | 9.3 (12.9) | 6.8 (6.9) | 19.8 |
| 2 | Proposed control | 10.0 (13.9) | 4.3 (4.4) | 18.3 |

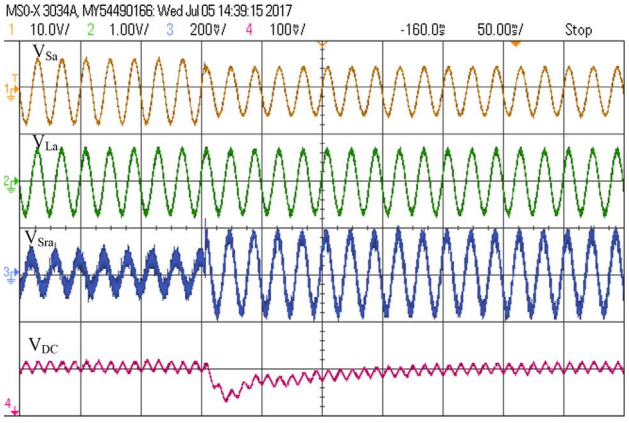


(a) Voltage waveforms during sag in supply voltage
Scale- $V_{Sa}$: 500 V/div., $V_{La}$: 500 V/div., $V_{Sra}$: 100 V/div., $V_{DC}$: 50 V/div., time: 50 ms/div.

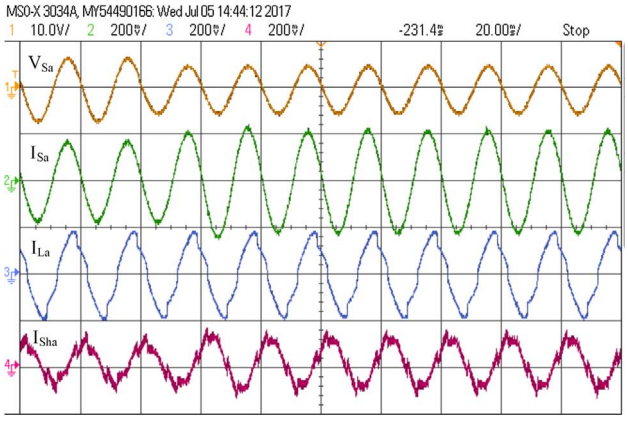


(b) Current waveforms during sag in supply voltage
Scale- $V_{Sa}$: 500 V/div., $I_{Sa}$: 100 A/div., $I_{La}$: 100 A/div., $I_{Sha}$: 100 A/div., time: 20 ms/div.

**Fig. 12.** Waveforms during sag in supply voltage.

reactive power of load. Source current waveforms in base case (without mean block) are shown in Fig. 10. It can be observed that in spite of unbalance compensation by shunt APF, certain amount of unbalance remains in source currents. On the contrary, source currents are found to be comparatively much balanced in proposed control (with mean block), as already shown in Fig. 7c. To assess power quality of these source currents unbalance and THD are considered for comparison. Source current power quality parameters are presented in Table 2. For comparing unbalance in three phase quantity, percentage unbalance parameter is proposed. Percentage unbalance can be computed using Eq. (31).

$$\%Unb = \frac{|I_{a,rms}-I_{b,rms}| + |I_{b,rms}-I_{c,rms}| + |I_{c,rms}-I_{a,rms}|}{I_{a,rms} + I_{b,rms} + I_{c,rms}} \times 100 \quad (31)$$

As evident from Table 2, proposed control performs better in compensating load current unbalance and harmonics. This betterment is due to reduction in ripples in output of PI controller by Mean block and thereby suppression of ripples in reference d-axis source current (Fig. 11).

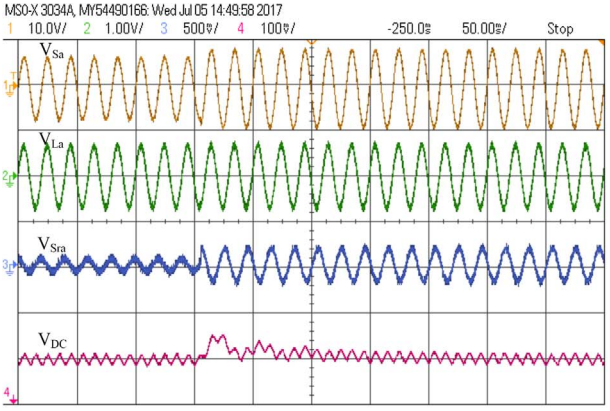


(a) Voltage waveforms during swell in supply voltage
Scale- $V_{Sa}$: 500 V/div., $V_{La}$: 500 V/div., $V_{Sra}$: 250 V/div., $V_{DC}$: 50 V/div., time: 50 ms/div.

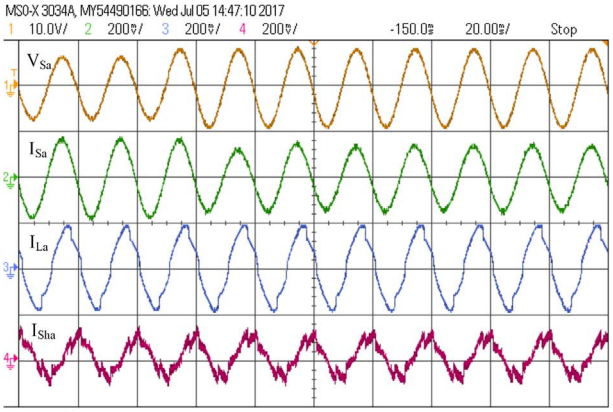


(b) Current waveforms during swell in supply voltage
Scale- $V_{Sa}$: 500 V/div., $I_{Sa}$: 100 A/div., $I_{La}$: 100 A/div., $I_{Sha}$: 100 A/div., time: 20 ms/div.

**Fig. 13.** Waveforms during swell in supply voltage.

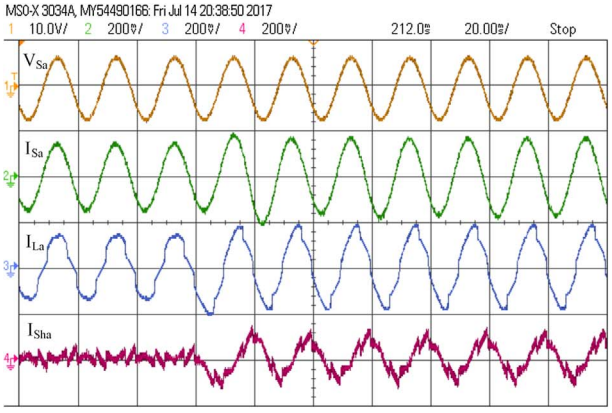


(a) Current waveforms during change in load
Scale- $V_{Sa}$: 500 V/div., $I_{Sa}$: 100 A/div., $I_{La}$: 100 A/div., $I_{Sha}$: 100 A/div., time: 20 ms/div.

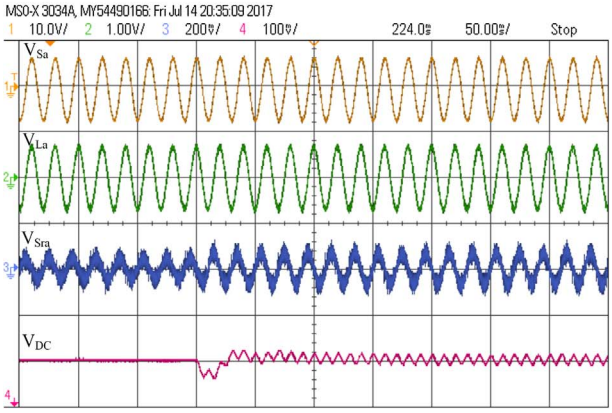


(b) Voltage waveforms during load change
Scale- $V_{Sa}$: 500 V/div., $V_{La}$: 500 V/div., $V_{Sra}$: 100 V/div., $V_{DC}$: 50 V/div., time: 50 ms/div.

**Fig. 14.** Waveforms during change in load.

Performance of proposed control in reducing overall VA loading of UPQC is presented in Table 3. Actual reactive power demand of load is 14.3 kVAr of which 10 kVAr is unbalanced and 4.3 is balanced. In base case where total reactive power demand is shared equally among two APFs, series APF supplies 6.8 kVAr, which is not exactly half of total reactive power due to tracking issues between reference and actual signals. Since series APF supplies balanced power, more than required, in some phases shunt APF has to consume reactive power to balance it with load. This leads to circulation of reactive power. Reactive power load on shunt APF is 9.3 kVAr. Since shunt APF also supplies some real power for compensating unbalance, VA burden is 12.9 kVA.

In proposed control, there is no circulation of reactive power, and total reactive power load on both APFs is equal to reactive power demand of the load. This reduces VA burden on UPQC by 7.6% in comparison to base case.

### 6.2. Performance during sag in supply voltage

Performance of proposed control is tested for sag of 25% in supply voltage (see Fig. 12). During this sag load voltage magnitude is maintained constant through injection of suitable voltage by series APF. On occurrence of sag, phase angle and magnitude of series voltage changes since an additional voltage component in phase with source voltage is to be supplied to compensate for sag. Due to in phase injection of series voltage, series APF delivers real power to grid, which leads to reduction in DC link voltage and undershoot of 32 V (4.6%) occurs. PI controller acts to bring DC link voltage back to steady state value within 0.15 s. Since load power remains constant, source current increases during sag.

### 6.3. Performance during swell in supply voltage

A voltage swell of 25% is created and performance of UPQC is observed (see Fig. 13). During the swell in source voltage, load voltage is maintained constant. Phase angle and magnitude of series voltage changes because now it has to supply a voltage component out of phase with source voltage to compensate for swell. Because of out of phase injection of voltage, series APF consumes real power from grid. This leads to overshoot of 26 V (3.7%) in DC link voltage, which is brought back to steady state by PI action within 0.15 s. Source current reduces to maintain constant power supply to load during swell.

### 6.4. Performance during change in load

To simulate load change, initially UPQC is operated with load - 1 & 2, and load-3 (unbalanced load) is switched ON, due to which load and source currents increase (see Fig. 14). Source current experiences some oscillations due to fluctuations in DC link voltage, but stabilizes in 0.07 s. Both, load voltage and current, stabilize in 0.01 s. Shunt APF current increases to compensate for load unbalance. DC link voltage goes through an undershoot of 17 V (2.4%) and stabilizes in 0.05 s. Series APF voltage increases because now it has to supply whole balanced reactive power. Rest of voltages remain unaffected.

### 6.5. Performance during unbalanced supply voltage disturbance

Performance of proposed UPQC$_{DG}$ is also validated during an

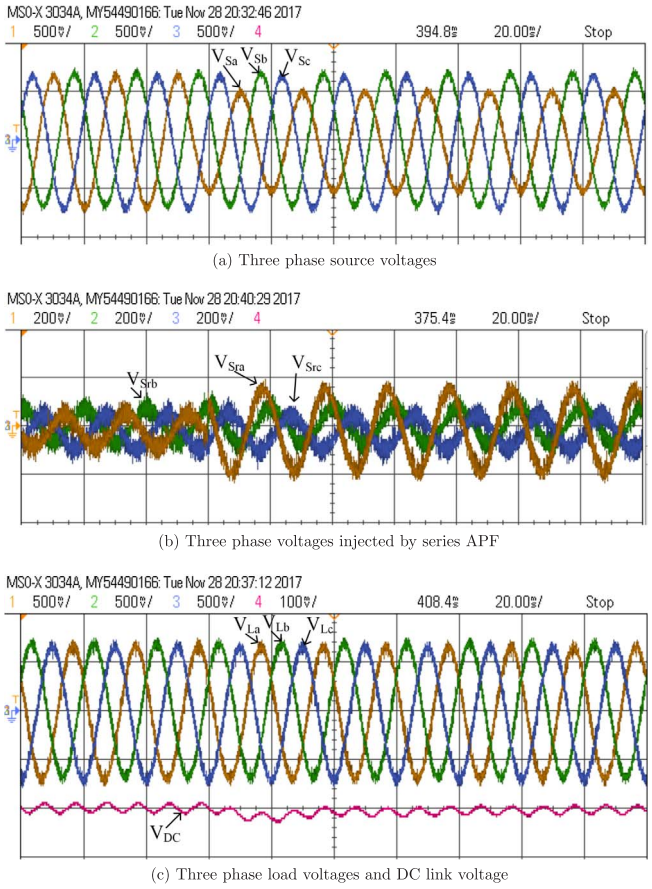


**Fig. 15.** Waveforms during unbalanced sag in supply voltage. Scale – $V_S$: 250 V/div., $V_{Sr}$: 100 V/div., $V_L$: 250 V/div., $V_{DC}$: 50 V/div., time: 20 ms/div.

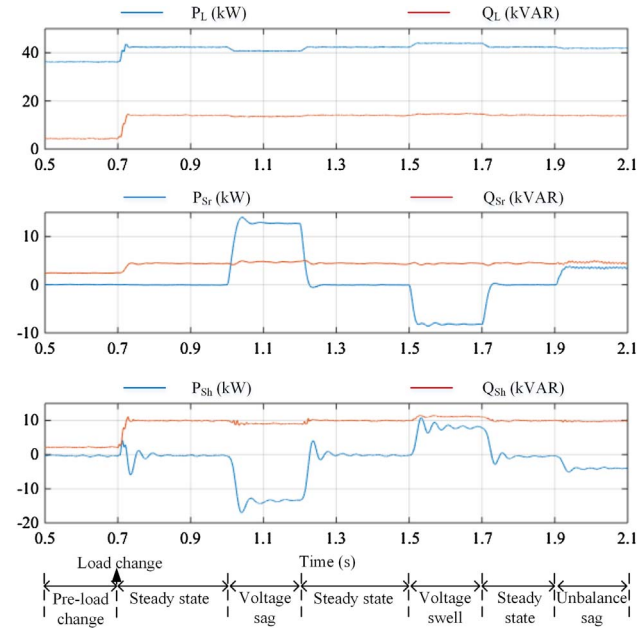


**Fig. 16.** Variations in real and reactive powers of different components during various modes of operation.

unbalanced source voltage disturbance (Fig. 15). A 25% sag is created in phase A of supply voltage, while voltages of other two phases remain constant. During this disturbance, series APF injects compensating unbalanced voltages, and maintains load voltages constant and balanced. DC link voltage remains constant except for minor undershoot. In comparison to three phase sag, the DC link undershoot is negligible in this case as expected.

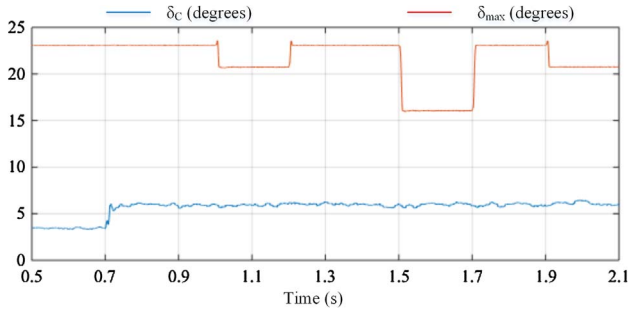


**Fig. 17.** Variations in power angle during various modes of operation.

### 6.6. Variations in power and power angle

As UPQC passes through various modes of operation, real and reactive powers associated with load, series APF and shunt APF change (Fig. 16). In pre-load change state, the unbalanced load is disconnected, so remaining loads consume balanced reactive power of 4.3 kVAR, which is shared equally between series and shunt APFs. At the instant of load change, unbalanced load is connected, which leads to increase in total real and reactive powers of load. Balanced reactive power demand remains 4.3 kVAR, which is supplied by series APF. Remaining reactive power (10 kVAR), which is unbalanced, is supplied by shunt APF. As discussed before, this scheme avoids reactive power circulation and overburdening of UPQC.

During voltage sag (three phase), series APF injects a component of voltage in phase with grid voltage (current), apart from supplying part of reactive power. This in-phase injection of component of series voltage leads to active power injection by series APF. Since, UPQC doesn't have any power source, this active power is taken from grid via shunt APF. Similar phenomenon occurs during unbalance sag, but amount of active power injected by series APF is less in comparison to three phase sag. During voltage swell, series APF injects a out of phase voltage component, which leads to consumption of active power by series APF. This active power is fed back to grid via shunt APF. During sag and swell reactive powers of both APFs remain same except slight variations.

Variation in power angle is shown in Fig. 17. Steady state value of $\delta_{max}$ is 23.1°. During sag and swell, $\delta_{max}$ value changes because of variation in per unit grid voltage ($f_S$). On other hand, $\delta_C$ changes from 3.5°to 6.0°, when load changes, since it is dependent on load real and reactive powers. Minimum of the $\delta_{max}$ and $\delta_C$ (which is $\delta_C$ in this case) is selected as final value of power angle ($\delta_F$).

## 7. Conclusions

In this paper, a new PAC method is proposed for control of UPQC in presence of unbalanced load. Proposed PAC method shares reactive power burden of load between series and shunt APF and effectively handles balanced and unbalanced loads. Proposed PAC method shares reactive power equally if unbalanced reactive power is less than half of total reactive power, otherwise, it provides total unbalanced reactive power burden to shunt APF and balanced reactive power to series APF. This approach avoids circulation of reactive power between two APFs of UPQC. During load unbalance, proposed PAC method results in VA loading of UPQC to be reduced by 7.6% in comparison to existing PAC, which shares reactive power equally in case of both balanced and unbalanced load. Another contribution of the paper is to add a running mean (moving average) block at the output of PI controller to improve power quality during unbalanced load. The mean block reduces effects of DC link voltage ripples, which are caused due to unbalanced load

compensation by UPQC. It is shown that frequency of mean block should be equal to frequency of DC link ripples for best results. When compared to conventional method, using mean block reduces source current unbalance from 2.66% to 0.11% and THD from 4.38% to 3.59%. Also, a percentage unbalance parameter is defined, based on which effectiveness of proposed method is validated. Dynamic performance of proposed PAC method has been tested during supply voltage disturbances and change in load. In face of these variations, quality power is supplied to load and supply currents are maintained balanced and undistorted, with unity power factor. Real time simulation is carried out in Opal-RT and results along with detailed analysis validate effectiveness of proposed method.

## Appendix A. FFT analysis of current

See Fig. A.18.

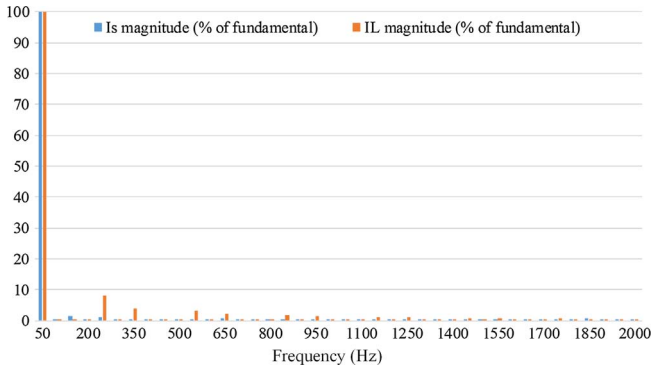


**Fig. A.18.** Frequency spectrum of source and load currents.

## Appendix B. Supplementary material

Supplementary data associated with this article can be found, in the online version, at http://dx.doi.org/10.1016/j.ijepes.2018.02.035.

## References

[1] Singh B, Chandra A, Al-Haddad K. Power quality: problems and mitigation techniques. John Wiley & Sons; 2014.
[2] Khadkikar V. Enhancing electric power quality using UPQC: a comprehensive overview. IEEE Trans Power Electron 2012;27(5):2284–97.
[3] Khadkikar V, Chandra A. UPQC-S: a novel concept of simultaneous voltage sag/swell and load reactive power compensations utilizing series inverter of UPQC. IEEE Trans Power Electron 2011;26(9):2414–25.
[4] Khadkikar V. Fixed and variable power angle control methods for unified power quality conditioner: operation, control and impact assessment on shunt and series inverter kVA loadings. IET Power Electron 2013;6(7):1299–307.
[5] Viji AJ, Victoire TAA. Enhanced PLL based SRF control method for UPQC with fault protection under unbalanced load conditions. Int J Electr Power Energy Syst 2014;58:319–28.
[6] Patel A, Chaturvedi P. Performance of SRF-UVTG based $UPQC_{DG}$ for integration of solar PV with non-linear loads. 2016 IEEE international conference on power electronics, drives and energy systems (PEDES). IEEE; 2016. p. 1–5.
[7] Devassy S, Singh B. Dynamic performance of solar PV integrated UPQC-P for critical loads. In: Proc. 12th IEEE INDICON; 2015. p. 1–6.
[8] Khadkikar V, Agarwal P, Chandra A, Barry A, Nguyen T. A simple new control technique for unified power quality conditioner (UPQC). In: Proc. 11th IEEE ICHQP; 2004. p. 289–93.
[9] Khadkikar V, Chandra A. A new control philosophy for a unified power quality conditioner (UPQC) to coordinate load-reactive power demand between shunt and series inverters. IEEE Trans Power Del 2008;23(4):2522–34.
[10] Senthilkumar A, Raj PA-D-V. ANFIS and MRAS-PI controllers based adaptive-UPQC for power quality enhancement application. Electr Power Syst Res 2015;126:1–11.
[11] Axente I, Ganesh JN, Basu M, Conlon MF, Gaughan K. A 12-kVA DSP-controlled laboratory prototype UPQC capable of mitigating unbalance in source voltage and load current. IEEE Trans Power Electron 2010;25(6):1471–9.
[12] Kesler M, Ozdemir E. Synchronous-reference-frame-based control method for UPQC under unbalanced and distorted load conditions. IEEE Trans Industr Electron 2011;58(9):3967–75.
[13] Limongi L, Roiu D, Bojoi R, Tenconi A. Analysis of active power filters operating with unbalanced loads. ECCE 2009. IEEE energy conversion congress and exposition, 2009. IEEE; 2009. p. 584–91.
[14] Dang P, Petzoldt J. A new control method for eliminating the 2nd harmonic at the DC link of a shunt APF under an unbalanced and nonlinear load. Proceedings of the 2011-14th European conference on power electronics and applications (EPE 2011). IEEE; 2011. p. 1–5.
[15] Patnaik N, Panda AK. Performance analysis of a 3 phase 4 wire UPQC system based on PAC based SRF controller with real time digital simulation. Int J Electr Power 2016;74:212–21.
[16] Panda AK, Patnaik N. Management of reactive power sharing & power quality improvement with SRF-PAC based UPQC under unbalanced source voltage condition. Int J Electr Power Energy Syst 2017;84:182–94.
[17] Parma GG, Dinavahi V. Real-time digital hardware simulation of power electronics and drives. IEEE Trans Power Del 2007;22(2):1235–46.
[18] Ould-Bachir T, Blanchette HF, Al-Haddad K. A network tearing technique for FPGA-based real-time simulation of power converters. IEEE Trans Ind Electron 2015;62(6):3409–18.